Assessing Manganese Efflux Using SEA0400 and Cardiac T_1-Mapping Manganese-Enhanced MRI in a Murine Model

B. Waghorn[1,2], Y. Yang[1], A. Baba[3], T. Matsuda[3], N. Yanasak[1], and T. C-C. Hu[1,2]

[1]Small Animal Imaging, Medical College of Georgia, Augusta, GA, United States, [2]NRE and Medical Physics Programs, Georgia Institute of Technology, Atlanta, GA, United States, [3]Graduate School of Pharmaceutical Sciences, Osaka University, Osaka, Japan

Introduction

The Na^+/Ca^{2+} exchanger (NCX) is involved in the regulation of intracellular cardiac Ca^{2+} concentration via either the forward (Ca^{2+} extrusion) or reverse (Ca^{2+} influx) mode. Up to 81% of Ca^{2+} efflux in mice occurs via the NCX (1). During the early phase of reperfusion following myocardial ischemia, the reverse mode of the NCX is activated and intracellular Ca^{2+} overloading takes place. The pathological increase in intracellular Ca^{2+} concentration leads to various cell injuries, which have successfully been reduced using a NCX inhibitor (2). SEA0400 (3), 2-[4-[(2,5-difluorophenyl) methoxy] phenoxy]-5-ethoxyaniline, is such a potent and selective NCX inhibitor, having been shown to provide protection from cardiac ischemia/reperfusion injury, from digitalis induced arrhythmia and myocardial stunning.

Monitoring strategies to assess the changes in Ca^{2+} flux *in vivo* could therefore be diagnostically important but are currently limited. One potential technique to monitor relative myocardial Ca^{2+} efflux is with a surrogate biomarker of Mn^{2+}. Producing cardiac T_1-maps at multiple time points post-$MnCl_2$ infusion allows *in vivo* washout curves to be produced and studied. The first part of the study was designed to examine the effect of varying the infusion dose of $MnCl_2$ on the washout rate. Secondly, NCX inhibitor SEA0400 was injected into the mice to examine the effect of inhibiting this efflux pathway on the Mn^{2+} efflux.

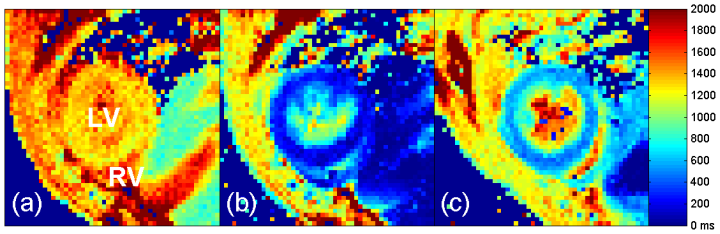

Figure 1. *Example short-axis mouse heart T_1-maps (a) pre-$MnCl_2$ infusion (b) 0.2 hours and (c) 5 hours post-$MnCl_2$ infusion.*

Methods

Manganese-enhanced MRI (MEMRI) experiments were performed in adult male C57Bl/6 mice (7-13 weeks old, 24.7±2.1g). The animals were anesthetized with a mixture of medical air, oxygen (1:1) and isoflurane and maintained at 1.0-2.7% isoflurane. $MnCl_2$ was infused into the tail vein at a rate of 0.6 ml/hr. For the dose dependent study $MnCl_2$ doses of 280, 190, 120 and 65 nmoles/g total body weight (BW) was infused into control mice. To study the effect of inhibiting the NCX a second study was performed. Each group was infused with 190 nmoles/g BW $MnCl_2$, with 50, 35, 20 or 10 mg/kg SEA0400 injected i.p. one hour post-$MnCl_2$ infusion. Images were acquired on a 7.0-T, 20-cm horizontal bore BioSpec MRI spectrometer (Bruker Instruments, Billerica, MA) equipped with a micro imaging gradient insert (950 mT/m). Animal setup procedures followed those previously described (4). A 35 mm inner diameter volume coil was used to transmit and receive at ^1H frequency. An ECG-gated, flow-compensated Look-Locker MRI pulse sequence was used to acquire both pre-$MnCl_2$ and post-$MnCl_2$ T_1-map short axis heart images, as previously described (5). The T_1-mapping parameters were as follows: matrix = 128 x 128; Inter-TE/TR = 2.5 ms/10 sec; slice thickness = 1.0 mm; FOV = 3.0 x 3.0 cm; NA = 2; inversion time/interval = 9/138 ms; echo images = 50; imaging time ~ 43 minutes. The T_1 value of each pixel was calculated in two steps using a custom written C^{++} program (5). Regions of Interest (ROI) analysis for the LV Wall was performed using AMIDE (6). The average regional T_1 value and ΔR_1 values were calculated, where ΔR_1 = (post-$MnCl_2$ infusion R_1) – (pre-$MnCl_2$ infusion R_1).

Results

Figure 1 shows sample cardiac short axis T_1-maps before $MnCl_2$ infusion (Figure 1a), 0.2 hours post- (Figure 1b), and 5 hours post- (Figure 1c) $MnCl_2$ infusion for a control mouse. Temporal changes in ΔR_1 for the $MnCl_2$ and SEA0400 dose dependent studies are shown as an approximation to the Mn^{2+} efflux rate determination in Figures 2a and 3a along with first order exponential fits. The dose dependence on the exponential half-life from these fits is displayed in Figures 2b and 3b. The half-lives range from 2.0 hrs to 9.5 hrs for the 280 nmoles/g BW and 65 nmoles/g BW groups, respectively. The 35 and 50 mg/kg SEA0400 group efflux half-life values are significantly different ($p < 0.05$) from the control group. The half life for the 50 mg/kg group was extended to 5.6±1.1 hrs.

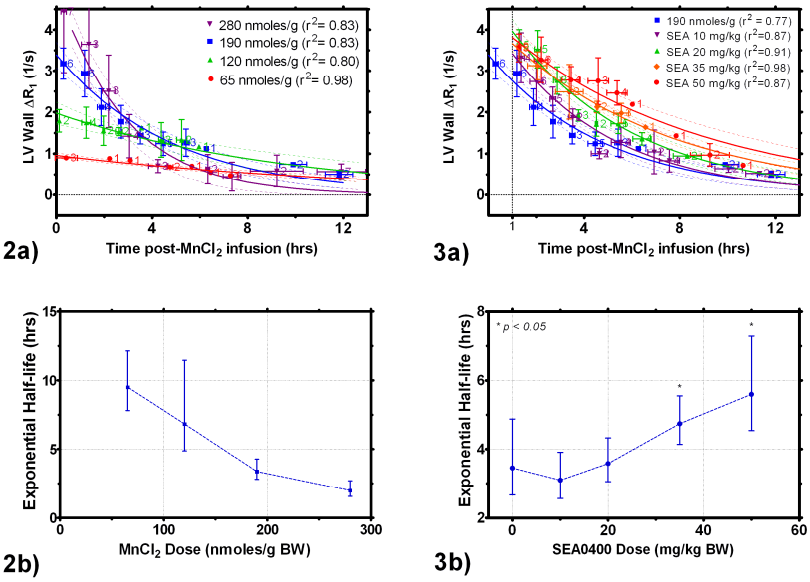

Figures 2 – 3. *Temporal ΔR_1 changes post-$MnCl_2$ infusion for (2a) dose dependent study and (3a) SEA0400 study. First order exponential fits and 95% CIs are shown. 2b) and 3b) show the dose dependence of the exponential half life.*

Conclusions

The MEMRI T_1-mapping protocol provides a quantitative means of measuring temporal changes in the LV Wall relaxation rate, allowing for the inferred study of Mn^{2+} efflux mechanisms non-invasively. There is a Mn^{2+} dose dependence on the ΔR_1 washout rate, with higher doses providing higher ΔR_1 at steady state initially along with a relatively rapid efflux rate. SEA0400 treatment has been shown to attenuate the Mn^{2+} washout rate. Above 20 mg/kg SEA0400 a significant increase in ΔR_1 washout half-life can be observed. Thus far MEMRI T_1-mapping has proved sensitive enough to detect NCX_i modulation fluctuations. Combining information from both studies could allow for individual efflux mechanisms and their relative rates to be determined. The rate of cardiac Mn^{2+} washout could suggest potential Ca^{2+} handling mechanisms, with alterations to the washout rate following inhibition of the NCX with SEA0400 allowing for estimates of the contribution of the different efflux components. Studying Mn^{2+} efflux using this MEMRI T_1-mapping protocol therefore would provide a pre-clinical murine model for examining alterations in Ca^{2+} efflux and to potentially monitor disease progression.

References

1. Antoons G,et al., *J Physiol* 2002; **543**; Pt 3: 889-898. **2.** Takahashi K, et al., *Eur J Pharmacol* 2003; **458**; 1-2: 155-162. **3.** Matsuda T, et al., *J Pharmacol Exp Ther* 2001; **298**; 1: 249-256. **4.** Waghorn BJ, Edwards T, Yang Y, Chuang KH, Yanasak N, Hu TC-C. *NMR Biomed* 2008; In Press. **5.** Chuang KH, Koretsky A. *Magn Reson Med* 2006; **55**; 3: 604-611. **6.** Loening AM, Gambhir SS. *Mol Imaging* 2003; **2**; 3: 131-137.